The multi-scale dissipative structures underlying granular geomaterials mechanics: *from theory to civil engineering practice*

E. FROSSARD

Consultant (*formerly Technical Director at Tractebel Engineering and Lecturer at Centrale Paris*) efrossard52@gmail.com

…

Résumé :

L'article, résultant d'un travail de long terme sur la physique des géomatériaux granulaires et le génie civil de grandes infrastructures, synthétise une nouvelle vision du comportement mécanique de ces matériaux, à partir d'une approche dissipative micro-mécanique originale. Après le contexte dans le génie civil et les hypothèses-clé, il présente les aspects essentiels des structures dissipatives induites par la friction de contact élémentaire, associée à des spécificités de mécanique statistique dans ces matériaux en mouvement quasi-statique, et leur expression multi-échelle par des relations tensorielles clé : les équations de la dissipation d'énergie résultant de la friction. Ces relations de dissipation et leurs conséquences, dûment validées par des données expérimentales étendues, sont la base des applications pratiques développées ensuite, résultant explicitement en un large ensemble de propriétés d'usage général en génie civil.

Bien que l'essentiel de l'article soit focalisé sur les caractères induits par la friction de contact, une dernière section présente d'autres propriétés-clé résultant de la rupture des granulats, autre processus dissipatif après la friction de contact. Ces propriétés incluent des incidences explicites sur les effets d'échelle dans le comportement structural d'ouvrages, vérifiées sur de grands ouvrages.

Abstract :

The paper, resulting from a long-term work into the physics of granular geomaterials, as well as into the engineering of large civil works, reviews and summarizes a new vision of granular geomaterials mechanical behavior, through an original micro-mechanical dissipative approach. After a section on civil engineering background and key assumptions, it begins on main theoretical features of dissipative structures induced by elementary contact friction, associated with specific statistical mechanics properties within granular materials in quasi-static motion, and their multi-scale expression into key tensor relations: the equations of energy dissipation resulting from contact friction. These dissipation relations and related features, duly validated by abundant experimental evidence, constitute the backbone of practical applications developed further on in the paper, resulting explicitly in a wide set of properties of general use in civil engineering.

Although most of the paper focusses on contact friction induced features, a last section presents other key features resulting from particle breakage, the other main dissipative process after contact friction.

These results include explicit incidences on size effects in civil works structural behavior, verified on large embankments.

Key words : granular geomaterials/ multi-scale approach/ civil engineering applications

1 Introduction- Key assumptions

Construction of large infrastructures commonly involves very large volumes of rockfill, up to tens of millions of cubic meters, as in rockfill dams, Figure 1. Because of difficulties and costs of relevant mechanical testing, design methods involving these materials include a large part of empirical extrapolation from past constructions. This situation has led recently to serious incidents during commissioning high dams worldwide, raising professional concern towards more rational design approaches. Present paper summarizes a long-term work to progress in that sense, proposing a new vision of these granular geomaterials mechanical behavior, through an original micro-mechanical dissipative approach, detailed extensively in a recent book [1].

Figure 1 – A large rockfill dam, and the typical rockfill used for its construction

Most of the paper develops multi-scale dissipative structures induced by elementary contact friction, and their expression by tensor equations of energy dissipation, resulting in a large set of macroscopic key properties relevant in geotechnical and civil engineering, including:

- The Failure Criterion, resulting into Coulomb criterion under critical state;
- The 3D stress-dilatancy relations between shear strength and volume changes;
- The Characteristic state, key to liquefaction phenomenon and its consequences;
- Cyclic Compaction features, widely used in materials improvement practice;
- Geostatic equilibrium (or coefficient K_0), key to braced excavations and shallow tunnels;

Last section presents other features resulting from particle breakage, the other main dissipative process after contact friction, including explicit incidences on size effects in shear strength, slope stability and safety factors, deformations and settlements in rockfill embankments.

Present paper being a synthesis, details and extensive proofs can be found in the reference book [1].

The multiscale approach presented in sections 2 to 8, was developed on the idea that granular geomaterials being densely discontinuous at small scale, macroscopic behavior is likely strongly conditional upon small scale behavior of intergranular contacts, and their irreversible energy

dissipation by contact friction. The granular media considered, under slow quasi-static motion, are constituted by rigid, cohesionless mineral particles, with randomly irregular but convex shapes. Interparticle contacts are unilateral, purely frictional with uniform friction, so there is no resistance to macroscopic tensile stresses. Relevant internal movements are contacts relative slidings, and relevant internal forces are contact forces resultants; internal work is done only by contact forces and contact slidings, and is fully dissipated. Macroscopic stresses considered are "effective stresses", with Soil Mechanics sign convention (compressive stresses and contraction strains noted as positive). In section 9 the mineral particles are no longer considered as rigid, but subject to crushing by fracture mechanics.

2 The tensor structures induced by contact friction

These structures are induced by contact friction conditioning specific "internal actions" tensors resulting from symmetric product between internal forces and internal movements, and holding the work rate of internal forces as first invariant, Table 1.

1] MATERIAL SET (in motion)	ELEMENTARY CONTACT	GRANULAR MASS	EQUIVALENT CONTINUUM
Scale	Microscopic	Mesoscopic	Macroscopic
	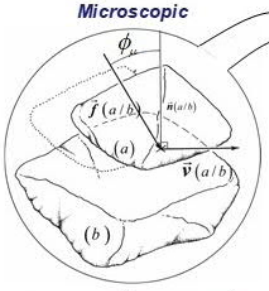	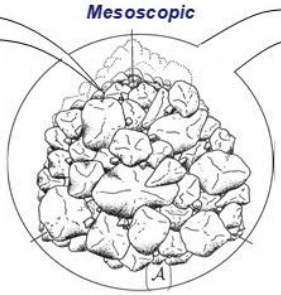	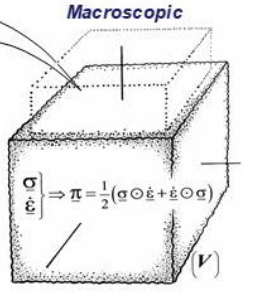
2] INTERNAL ACTIONS (2nd order symmetric tensors)	$\mathbf{p}(a/b)=\frac{1}{2}\left\{\vec{f}\otimes\vec{v}+\vec{v}\otimes\vec{f}\right\}$	$\mathbf{P}(\mathcal{A})=\sum_{\mathcal{A}(a<b\leq N)}\mathbf{p}(a/b)$	$\boldsymbol{\pi}=\frac{1}{2}\{\boldsymbol{\sigma}\otimes\dot{\boldsymbol{\varepsilon}}+\dot{\boldsymbol{\varepsilon}}\otimes\boldsymbol{\sigma}\}$ contracted
Work rate of internal forces	$\dot{W}(a/b)=\vec{f}\bullet\vec{v}=Tr\{\mathbf{p}(a/b)\}$	$\dot{W}(\mathcal{A})=\sum_{\mathcal{A}}\dot{W}(a/b)=\sum_{\mathcal{A}}\vec{f}\bullet\vec{v}=Tr\{\mathbf{P}(\mathcal{A})\}$	$\dot{\boldsymbol{\omega}}=\sum_{i,j}\sigma_{ij}\dot{\varepsilon}_{ij}=Tr\{\boldsymbol{\pi}\}$
3] ENERGY DISSIPATION due to friction	$Tr\{\mathbf{p}(a/b)\}=\sin\phi_\mu\,.N\{\mathbf{p}(a/b)\}$ with $\begin{cases}N\{\mathbf{p}\}=\lvert p_1\rvert+\lvert p_2\rvert+\lvert p_3\rvert=\lVert\vec{f}\rVert\cdot\lVert\vec{v}\rVert\\ \{p_1,p_2,p_3\}\ \text{eigen values of}\ \mathbf{p}(a/b)\end{cases}$	$Tr\{\mathbf{P}(\mathcal{A})\}=\sin\phi_\mu^{*}\,.N\{\mathbf{P}(\mathcal{A})\}$ with $\sin\phi_\mu^{*}=\frac{\sin\phi_\mu}{1-R(\mathcal{A}).(1-\sin\phi_\mu)}$, $R(\mathcal{A})=\frac{1}{(1-\sin\phi_\mu)}\cdot\left[1-\frac{N\{\sum_{\mathcal{A}}\mathbf{p}(a/b)\}}{\sum_{\mathcal{A}}N\{\mathbf{p}(a/b)\}}\right]$, Satisfies $0\leq R(\mathcal{A})\leq 1$	$Tr\{\boldsymbol{\pi}\}=\sin\phi_\mu^{*}.N\{\boldsymbol{\pi}\}$ in case of coaxiality, results in : $\sum_i\sigma_i\dot{\varepsilon}_i=\sin\phi_\mu^{*}.\sum_i\lvert\sigma_i\dot{\varepsilon}_i\rvert$

Table 1: Synopsis of multi-scale tensor structures induced by contact friction

At microscopic scale, i.e. the elementary sliding intergranular contact between two particles, Table 1, classical Coulomb friction laws linking basic contact friction ϕ_μ with contact force and relative sliding velocity, result in vector expression of energy dissipation rate due to friction:

$$\vec{f}(a/b)\bullet\vec{v}(a/b)=\sin\phi_\mu\cdot\left\|\vec{f}(a/b)\right\|\cdot\left\|\vec{v}(a/b)\right\| \qquad (1)$$

Both sides occur to be two first order invariants of elementary contact "internal actions" tensor **p**(a/b) resulting from symmetric tensor product of our two vectors: the *Trace* (scalar product of the vectors), and the sum of absolute values of eigen values (product of the vectors Euclidian norms), which is a tensor norm *N*, piecewise linear, with octahedron as unit ball. Thus, Coulomb contact friction laws induce between eigen values of **p**(a/b) a simple energy dissipation relation, piecewise linear:

$$Tr\{\mathbf{p}(a/b)\}=\sin\phi_\mu\,.N\{\mathbf{p}(a/b)\} \qquad (2)$$

At mesoscopic scale, the discontinuous granular mass, Table 1, is considered as a statistical population of moving contacts, the global work rate of internal forces being the sum of work rates developed by all contact forces. So, the relevant internal actions tensor **P**(*A*) is here the sum of all the tensors of elementary contacts internal actions, and its eigen values occur also to be linked by a dissipation relation induced by friction, but including here a specific population effect:

$$Tr\left\{\mathbf{P}(A)\right\} = \frac{\sin\phi_\mu}{1-R(A).(1-\sin\phi_\mu)}.N\left\{\mathbf{P}(A)\right\} \quad (3)$$

where function *R(A)*, holding this population effect, results from some energy exchanges between neighboring moving contacts, and is also related to the degree of disorder within the statistical distribution of moving contacts orientations. This function, comprised between 0 and 1, has been called "Internal feedback", Table 1. Naming "apparent intergranular friction" the material parameter:

$$\sin\phi_\mu^{\ *} = \frac{\sin\phi_\mu}{1-R(A).(1-\sin\phi_\mu)} \quad (4)$$

then, the dissipation relation in the granular mass in motion becomes:

$$Tr\left\{\mathbf{P}(A)\right\} = \sin\phi_\mu^{\ *}.N\left\{\mathbf{P}(A)\right\} \quad (5)$$

formally similar to the relation of elementary contact (2), however including here a population effect. The lower bound *R(A)*=0 corresponds to theoretical minimal dissipation solutions, which consist in fully polarized patterns in the distribution of moving contact orientations in the granular mass, Figure 2, consisting in two 3 D modes with signatures (+,-,-) and (+,+,-), separated by a plane strain border mode (+,0,-), which can be associated to their equivalent continuum strain modes. In plane strain condition, this pattern coincides with Rankine's slip lines concept (1857, [2]).

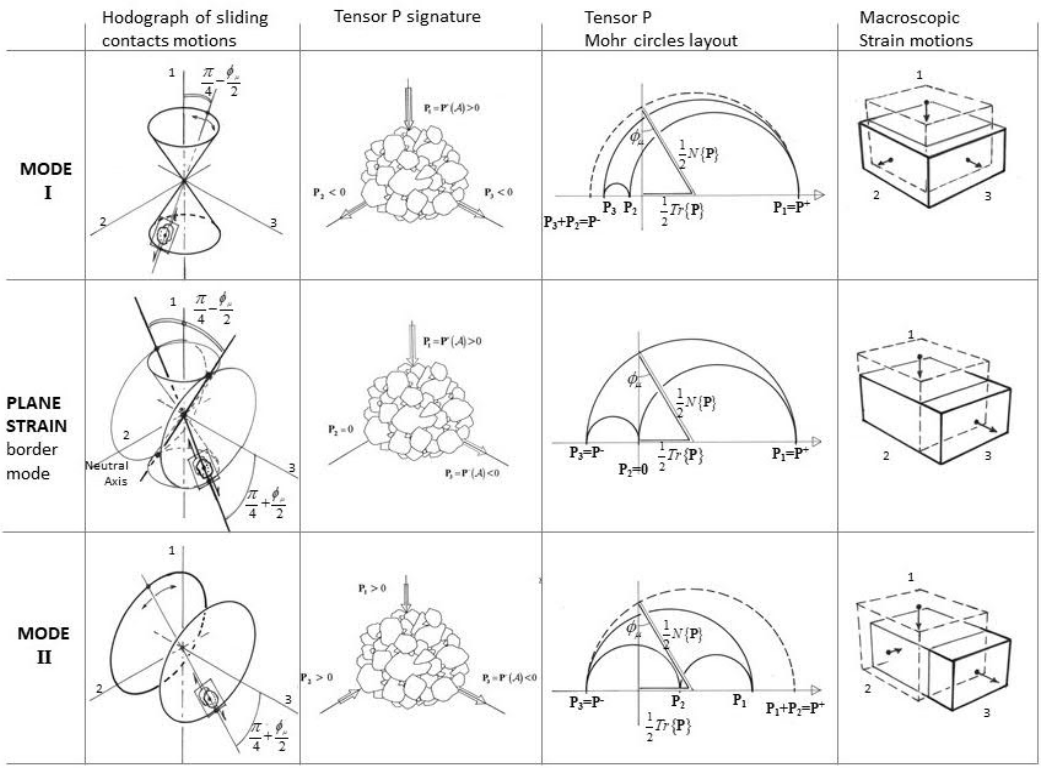

Figure 2 Theoretical minimal dissipation solutions

These results, combined with experimental data, suggest that the granular mass satisfies a "minimum dissipation rule" stating: *under regular, monotonic, quasi-equilibrium boundary conditions, the moving medium tends toward a regime of minimum energy dissipation compatible with imposed*

boundary conditions; and independent of the initial particular conditions; it was shown [1] to be a corollary of the Prigogine minimum entropy production theorem [3]. Usual granular media practice led to consider some neighbourhood around the theoretical minimum, with small values of *R(A)*<1, and $\sin\phi_\mu^*$ <1 considered as a material constant, in this neighbourhood of minimal dissipation.

At macroscopic scale, i.e. the equivalent continuum, Table 1, the "internal actions" $\boldsymbol{\pi}$ is defined here as contracted symmetric product between stress tensor $\boldsymbol{\sigma}$ (internal forces) and strain rate tensor $\dot{\boldsymbol{\varepsilon}}$ (internal movements), and our key assumptions do result in complete equality between average values of internal actions within discontinuous granular mass, and corresponding equivalent continuum. So, the same dissipation relation is verified:

$$Tr\{\boldsymbol{\pi}\} = \sin\phi_\mu^*.N\{\boldsymbol{\pi}\} \qquad (6)$$

When simple coaxiality is verified between stress and strain rate tensors (i.e. having same set of principal directions, but independent rankings of corresponding eigen values), above dissipation relation becomes in natural basis, confirming early work on the subject [4]:

$$\sum_i \boldsymbol{\sigma}_i\dot{\boldsymbol{\varepsilon}}_i = \sin\phi_\mu^*.\sum_i\left|\boldsymbol{\sigma}_i\dot{\boldsymbol{\varepsilon}}_i\right| \qquad (7)$$

Numbering principal directions according to principal stress ranking, $\boldsymbol{\sigma_1} \geq \boldsymbol{\sigma_2} \geq \boldsymbol{\sigma_3} > 0$ (normal stresses shall be compressive), analysis of dissipation equation (7) solutions leads to 6 allowed strain modes, according to the signature of the strain rates eigen values $(\dot{\boldsymbol{\varepsilon}}_1, \dot{\boldsymbol{\varepsilon}}_2, \dot{\boldsymbol{\varepsilon}}_3)$. It means that equation (7) provides a unified 3D description of what is usually called "loading-unloading" behavior in elasto-plastic approaches of granular materials, but here without requiring a different behavior formulation for "loading" motion and for "unloading" motion. A reversal in motion is seen here as a simple switch between different allowed strain modes obeying the same dissipative process, although explicit corresponding algebraic formulation will change from one strain mode to another because of the absolute values in equation (7). Experimental validations detailed later (section 6), including cyclic shear tests with motions reversals under various conditions, do clearly confirm this point of view.

3 Natural compatibility with heterogeneity: strain localization

Under regular boundary conditions and motion sufficiently close to minimum dissipation, this proximity of a minimum, and the peculiarities of terms on both sides of dissipation relation, result in the compatibility of internal actions with the mechanical heterogeneity of the medium: the dissipation relation (6) is satisfied by local variables as well as by average macroscopic values of the same variables, in spite of their strong local fluctuations. A similar property has been shown regarding stress and strain rates heterogeneity, with specific conditions on covariances of local fluctuations.

The allowed heterogeneities occur to represent quite well the known patterns of strain localization, Figure 3, including detailed shear bands theoretical internal structure, validated by experimental results [5], where the shear strain rate decreases exponentially with distance to band axis, locus of maximum shear:

$$\dot{\boldsymbol{\gamma}}(x) \approx \dot{\boldsymbol{\gamma}}(0).\exp(-k|\boldsymbol{x}|)\ ;\ with\quad k \approx \frac{1}{5\bar{d}}\mathrm{Ln}\left\{2\left[\frac{1+\sin\phi_\mu}{R\left(1-\sin\phi_\mu\right)}-1\right]\right\} \qquad (8)$$

Considering the localization process as a particular mode of heterogeneity growth in the motion, induced by the minimum dissipation rule, a localization criterion has been established, based on the non-convexity of the specific energy dissipation rate. One of its main consequences is that shear bands evolution tends to maximize the variance of deformation amplitude, i.e. predicting evolution towards the progressive concentration of shear motion in a quasi-discontinuity, usually called a "failure line".

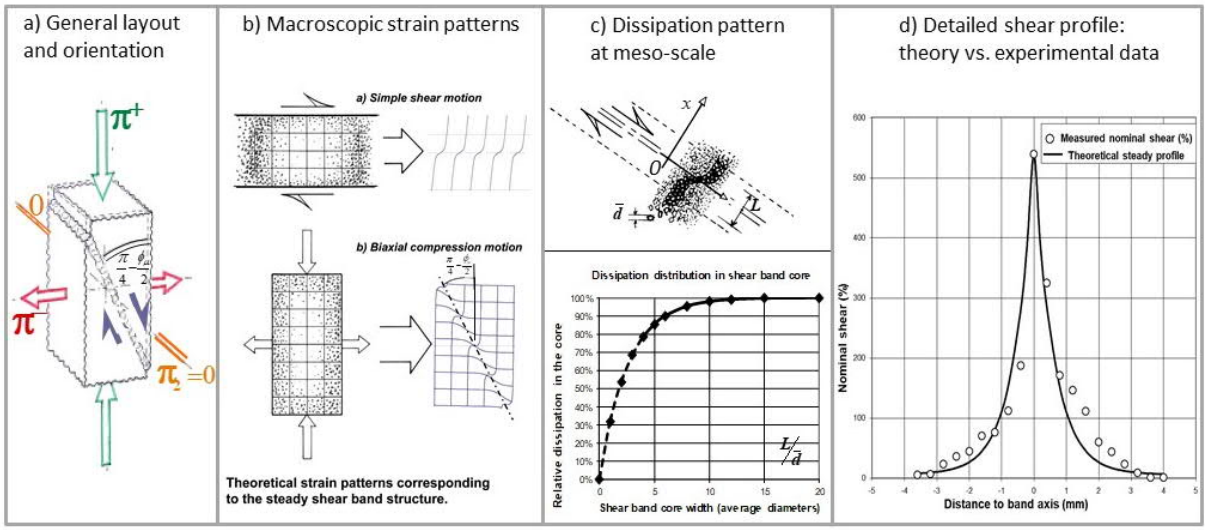

Figure 3 Strain localization: detailed features of theoretical steady shear band solution

4 A micromechanical basis of Coulomb failure criterion

Since historical publication of C.A. Coulomb in 1773 [6], the empirical criterion now called "Coulomb Failure Criterion" emerged progressively, and stood out as a reference in Soil Mechanics to characterize efficiently the mechanical behavior at macro-scale of frictional geomaterials, playing a key role in numerous methods for design and verification of civil engineering works, including slope stability, retaining structures and foundations. However, a direct link of general reach between this criterion and micro-mechanical features in granular materials, still remains to be established.

In granular geomaterials, densely discontinuous at small scale, the concept of "failure criterion" has to be related either to stress conditions providing a maximum of shear resistance, or to stress conditions making possible very large strains. This last feature of very large monotonic shear strains, shall be associated with stationary specific volume conditions of motion, as specific volume cannot vary indefinitely: the "critical state" conditions [7].

In the present approach, such a "failure criterion" has been analysed at critical state, associating dissipation equation (7) and stationary specific volume condition, and searching the deviatoric relation between deviatoric parameters $b = \frac{\boldsymbol{\sigma}_2 - \boldsymbol{\sigma}_3}{\boldsymbol{\sigma}_1 - \boldsymbol{\sigma}_3}$ (with $0 \le b \le 1$ under numbering convention $\boldsymbol{\sigma}_1 \ge \boldsymbol{\sigma}_2 \ge \boldsymbol{\sigma}_3 > 0$) and $c = \frac{\dot{\boldsymbol{\varepsilon}}_2 - \dot{\boldsymbol{\varepsilon}}_3}{\dot{\boldsymbol{\varepsilon}}_1 - \dot{\boldsymbol{\varepsilon}}_3}$, achieving a minimum of shear strength. Detailed analysis of all allowed strain modes, results in Coulomb criterion pyramid, built with the angle ϕ_μ^*, and generally associated with plane strain on intermediate principal direction, Figure 4a) and b):

$$\frac{\boldsymbol{\sigma}_1}{\boldsymbol{\sigma}_3} = \frac{Sup(\boldsymbol{\sigma}_1, \boldsymbol{\sigma}_2, \boldsymbol{\sigma}_3)}{Inf(\boldsymbol{\sigma}_1, \boldsymbol{\sigma}_2, \boldsymbol{\sigma}_3)} = \frac{1+\sin\phi_\mu^*}{1-\sin\phi_\mu^*} \qquad (9)$$

Although our initial assumption considers general (disordered) simple coaxiality, the set of minimal solutions constituting this failure criterion are found to achieve fully ordered coaxiality, it is also the only set of solutions achieving convexity of the failure criterion.

Considering critical state as an asymptotic regime, assuming a deviatoric relation f(*b*,*c*)=0 with some small deviations from above asymptotic minimal solution, results in a failure criterion with rounded apexes, Figure 4 c) and d), not far from shapes of experimental failure criterions measured long ago in extensive 3D testing [8] displaying similar slight undulations in some diagrams.

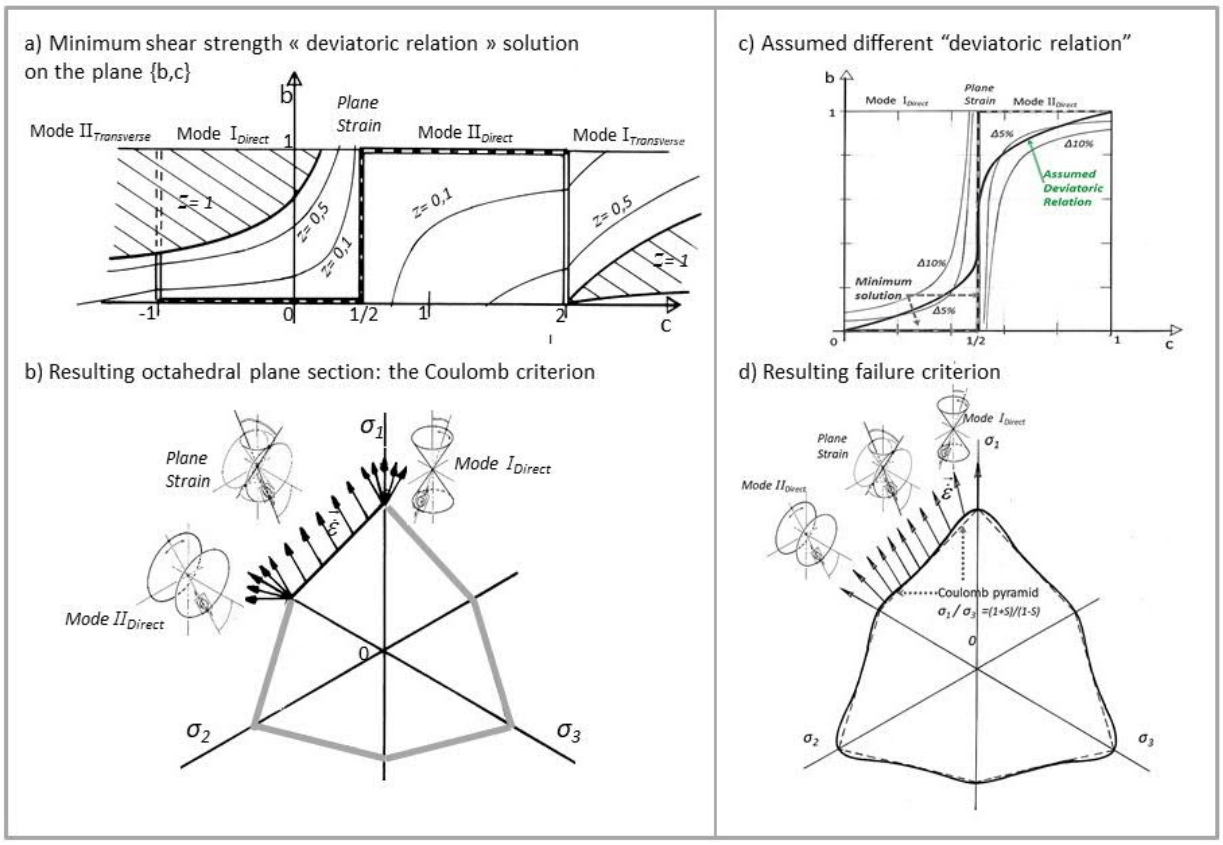

Figure 4-Failure criterion at critical state: least shear strength solution, incidences of small deviations (with corresponding micro-scale motion polarization features)

5 Coupling between shear strength and volume changes

Coupling between shear strength and volume changes in granular geomaterials plays a key role in mechanical characteristics used in civil engineering: on one side the loose state materials which tend to contract under shear, can develop under alternate shear motion in water-saturated conditions the feared phenomenon of liquefaction; on other side the densest state materials, which tend to dilate strongly (up to 25%) under shear motion, present drained shear strengths up to typically twice the value observed under loose state, justifying the compaction efforts developed in construction procedures.

In the present approach, this coupling has been analyzed in general 3D conditions for the relevant strain modes, by defining an index for these volume changes, the generalized dilatancy rate ***d***:

$$\begin{cases} \textit{When } \dot{\boldsymbol{\varepsilon}} \textit{ not null, then } \boldsymbol{d} = \dfrac{N\{\dot{\boldsymbol{\varepsilon}}\} - Tr\{\dot{\boldsymbol{\varepsilon}}\}}{N\{\dot{\boldsymbol{\varepsilon}}\} + Tr\{\dot{\boldsymbol{\varepsilon}}\}} \\ \boldsymbol{d} > 1 \Leftrightarrow \textit{dilatancy} \; ; \; 0 < \boldsymbol{d} < 1 \Leftrightarrow \textit{contraction} \end{cases} \qquad (10)$$

The dissipation equation (7) lays for each strain mode an analytical relation between between principal stress ratio σ_1/σ_3, deviatoric parameters of stresses and strain rates *b* and *c*, and generalized dilatancy rate *d*, constituting the generalized 3D stress-dilatancy relations for the corresponding strain modes.

As an example, for Mode I with signature (+,-,-), the analytical expression of ***d*** is $d = 1 - \dfrac{\dot{\boldsymbol{\varepsilon}}_v}{\dot{\boldsymbol{\varepsilon}}_1}$, and the generalized stress-dilatancy relation resulting from dissipation equation is:

$$\begin{cases} \dfrac{\boldsymbol{\sigma_1}}{\boldsymbol{\sigma_3}} = \left(\dfrac{1+S}{1-S}\right)\cdot\left\{ d + b\cdot\dfrac{\left[d-c(1+d)\right]\cdot\left[d\cdot\left(\frac{1+S}{1-S}\right)-1\right]}{\left[(2-c)-b\cdot\left[d-c(1+d)\right]\cdot\left(\frac{1+S}{1-S}\right)\right]}\right\} \\ With \quad -d \le c \le \dfrac{d}{1+d} \quad and \quad 0 \le b < \left(\dfrac{1-S}{1+S}\right)\cdot\dfrac{(2-c)}{\left[d-c(1+d)\right]} \;;\; S = \sin\phi_\mu^* \end{cases} \qquad (11)$$

For axisymmetric stress states (b=0) this generalized relation (11) reduces explicitly to classical Rowe stress-dilatancy relation [9], one of the most quoted key features of granular media behavior:

$$\frac{\boldsymbol{\sigma_1}}{\boldsymbol{\sigma_3}} = \boldsymbol{d}\cdot\left(\frac{1+\sin\phi_\mu^*}{1-\sin\phi_\mu^*}\right) = \left(1-\frac{\dot{\varepsilon}_v}{\dot{\varepsilon}_1}\right)\cdot\tan^2\left(\frac{\pi}{4}+\frac{\phi_\mu^*}{2}\right) \quad (for\ b=0, Mode\ I) \qquad (12)$$

The above shows that shear strength may vary strongly between peak strength and critical state, due to volume changes. As volume contraction during motion is a key to susceptibility to liquefaction effects, this coupling raises a question of practical interest: is there a definite limit between stress states inducing volume contraction, and those inducing dilatancy? This limit, named "Characteristic state" has been investigated for all allowed strain modes, analyzing both necessary conditions and sufficient ones to get volume contraction (and similarly for dilatancy) in the dissipation equation (7). The result is that a "characteristic state" do exist, coinciding with the pyramid of critical state Coulomb criterion: any motion under stress states remaining inside of this limit, will generate volume contraction.

Detailed analysis of generalized stress-dilatancy relations sets also that peak least shear strength criterion corresponds to the critical state Coulomb Criterion enlarged by peak dilatancy rate (d_{Max}):

$$\left(\frac{\boldsymbol{\sigma_1}}{\boldsymbol{\sigma_3}}\right)_{Peak} = \left(\frac{1+\sin\phi_\mu^*}{1-\sin\phi_\mu^*}\right)\cdot\boldsymbol{d}_{Max} \qquad (13)$$

Eventual deviations from this minimal solution can be assessed in a similar way as in above section 4. A synopsis of main global features resulting from this coupling between shear strength and volume changes, is displayed on Figure 5.

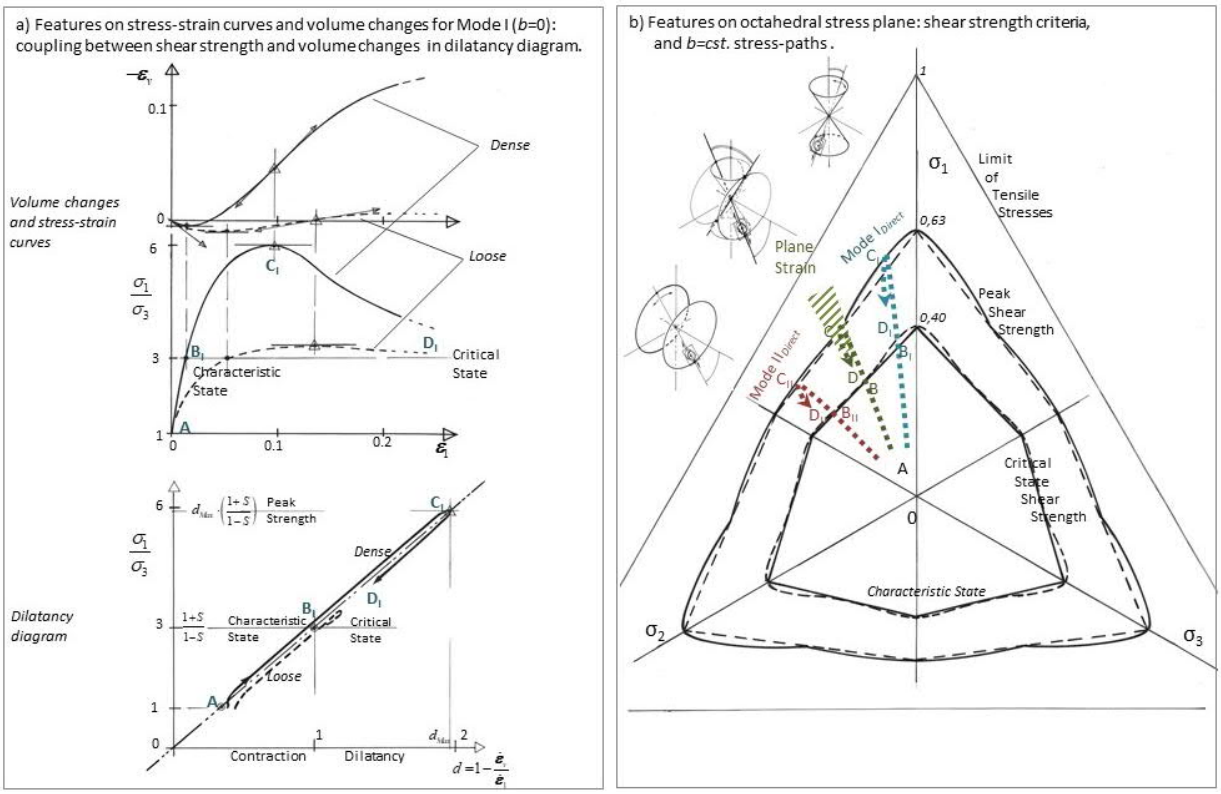

Figure 5- Synopsis of coupling between shear strength and volume changes global features

6 Experimental validations

A wide set of experimental validations is detailed in [1], resulting mainly from past independent experimental data, re-interpreted through the present approach of dissipative structures induced by friction, covering all kinds of experimental tests, either under monotonic or cyclic motion.
In particular, an outstanding publication [10] reports cyclic tests on Japanese Toyoura sand, either under cyclic triaxial test conditions, or under cyclic torsional shear tests performed on hollow cylinders, reporting tests results on special coordinates dilatancy diagrams. The dissipation equation (7) allows to foreseen theoretical trajectories on these special coordinates for alternate motions corresponding to the cyclic tests. These theoretical envelopes, adjusted to material parameter S=0,445 (i.e. ϕ_μ^* =26,4°), are in quite good agreement with data, Figure 6. Note that the same material parameter appears valid either for cyclic triaxial or cyclic torsional shear, here on dense Toyoura sand. The same publication displays also results for loose Toyoura sand: the results are again quite similar as for dense sand, and same theoretical curves adjust to experimental data with similar quality of fit.

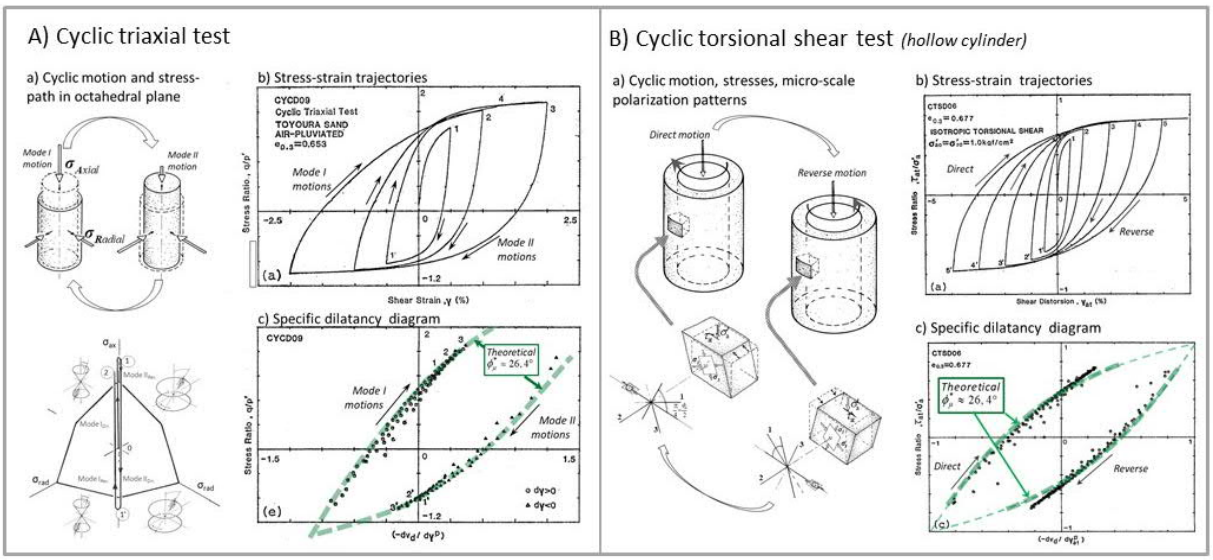

Figure 6- Theoretical envelopes on dilatancy diagrams of cyclic tests data *(after Pradhan et al. 1989)*

7 Cyclic compaction under small alternate shear strains

Granular materials compaction under alternate shear motion, Figure 7, is commonly experienced in daily life with usual granular materials of all kinds; it widely used in Civil Works for improving consistence of granular fills used as infrastructure platforms. by means of static or vibratory roller compactors. It is also responsible of liquefaction effects in saturated granular materials subject to earthquakes dynamic solicitations. A simplified model of this phenomenon is possible through the dissipation equation (7) under quasi-static conditions in the situation of simple shear under plane strain conditions, for small strain-driven alternate shear motion cycles. Main results are, Figure 7, a cyclic compaction in all situations, with best efficiency in the core of "Characteristic state":

$$\textit{Cyclic compaction ratio}\ \frac{\oint \dot{\varepsilon}_v}{\oint |\dot{\gamma}|} = \frac{4S}{(1-S^2)} \cdot \frac{\left(\frac{\sigma_1}{\sigma_3}\right)}{\left[\frac{\sigma_1}{\sigma_3}+\left(\frac{1-S}{1+S}\right)\right]\cdot\left[\frac{\sigma_1}{\sigma_3}+\left(\frac{1+S}{1-S}\right)\right]}\ ;\ \textit{energy efficiency}\ \ \frac{\oint \dot{\varepsilon}_v}{\oint \dot{\boldsymbol{\omega}}} = \frac{2}{\sigma_1+\sigma_3} \qquad (14)$$

and regarding energy efficiency, for low mean stresses, in agreement with "good practice" procedures

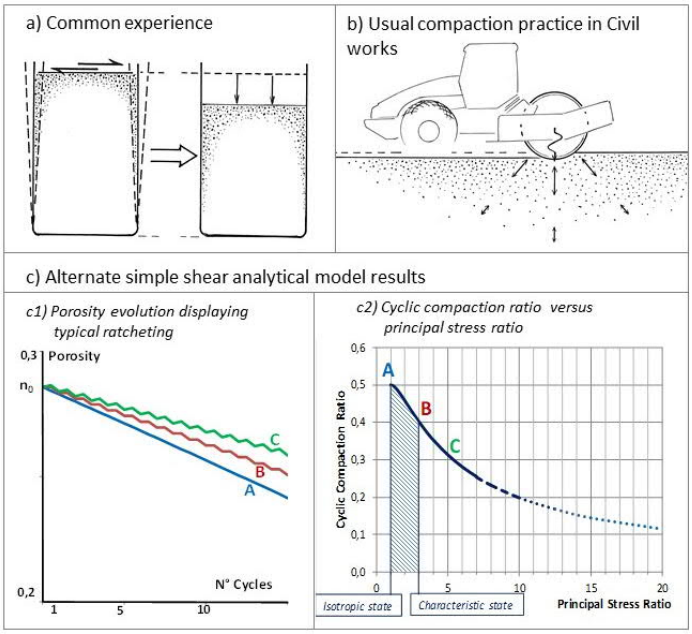

Figure 7- Cyclic compaction under alternate simple shear motion

8 Geostatic equilibrium: the K_0 effect

In the design of civil infrastructures such as roadways trenches in "cut and cover" and other retaining works for deep excavations or underground works, such as access shafts for underground works of Figure 8a), appears frequently the ratio "Coefficient of earth pressure at rest K_0", featuring the in situ geostatic equilibrium conditions by $K_0=\boldsymbol{\sigma}_h/\boldsymbol{\sigma}_v$, the ratio between horizontal and vertical principal stresses. Professionals commonly use the empirical Jaky formula (1948), initially published for the design of silos. Present micro-mechanical dissipative approach provides also an answer to the process of geostatic stress building, involving a global motion solution resulting from the combination of local movements, separately near the minimal dissipation, setting the macroscopic relation:

$$K_0 = \frac{\boldsymbol{\sigma_h}}{\boldsymbol{\sigma_v}} \approx \frac{1-\sin\phi_\mu^*}{1+\sin\phi_\mu^*} \qquad (15)$$

With typical values for dense to medium dense sands, the comparison with Jaky formula, Figure 8b), appears in fairly good agreement with commonly used values.

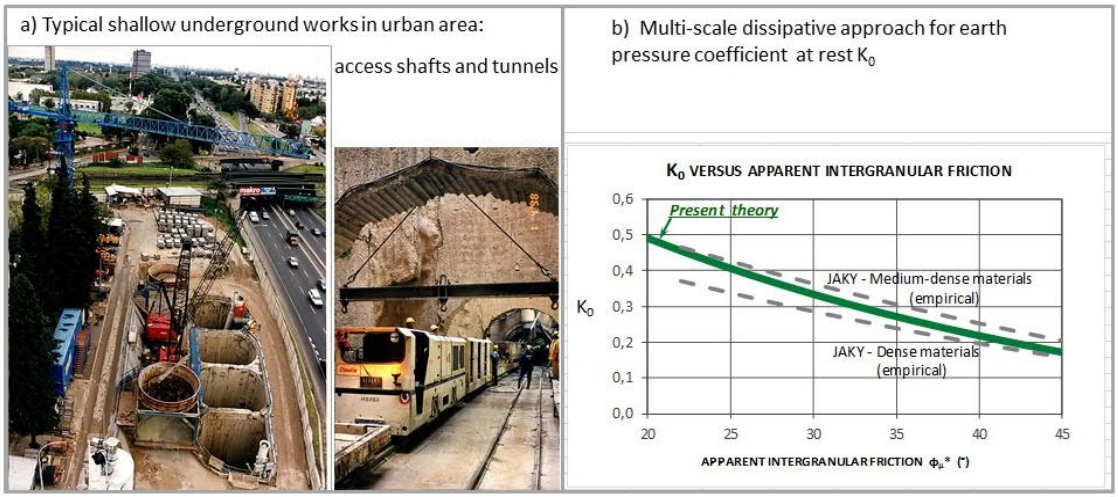

Figure 8- Design of civil works and geostatic equilibrium coefficient K_0

9 Scale effects due to grain breakage: practical applications to design and construction

When the mineral particles can no longer be considered as fully rigid, other dissipative effects due to grain breakage appear in the behavior, leading to curved experimental shear strength envelopes, effect more marked for coarse materials such as rockfill. These particle breakages have been shown to induce significant scale effects in macroscopic shear strength, through a simple model related to fracture mechanics, as particles fail mostly by tensile Mode I of fracture mechanics, with statistical distribution of crushing strengths ruled by Weibull statistics, with a specific material parameter *m*.
This results in a proved "Scale Effect Rule" operating on shear strength envelopes [11]: considering two granular materials M_0 and M_1 produced by the same homogeneous mineral stock, compacted to the same initial density, with geometrically similar gradation curves G_0 and G_1, characterized by a "characteristic diameter "D_0 and D_1 (for instance D_{Max}), their shear strength envelopes are linked by:

$$\tau_0 = f_0(\sigma_n) \quad \Rightarrow \quad \tau_1 = \left(\frac{D_1}{D_0}\right)^{\frac{-3}{m}} \cdot f_0\left\{\sigma_n \cdot \left(\frac{D_1}{D_0}\right)^{\frac{3}{m}}\right\} \tag{16}$$

Sets of test compilations interpreted by this approach, have led to assess a "central trend shear strength envelope" for small size rockfills with maximum stone diameter 0,15m, with a power formulation:

$$\begin{cases} \text{for } D_{Max} = 0{,}15m \quad \tau \approx 3{,}5 \cdot \sigma_n^{\,0{,}80} \quad \tau \text{ , } \sigma_n \text{ in kPa} \\ \text{for } D_{Max} \neq 0{,}15m \; \tau \approx 3{,}5 \cdot \left(\frac{0{,}15}{D_{Max}}\right)^{0{,}1} \cdot \sigma_n^{\,0{,}80} \end{cases} \tag{17}$$

Above Scale Effect Rule allows the implementation of a rational method to evaluate the shear strength envelope of a given large size rockfill, on the basis of tests performed on gravel sized reduced granular fill similar to the rockfill, produced from the same mineral stock. It allows also to analyse combined effects of coarse gradations, steeper slopes, and higher embankments, on the stability of embankments against shear failure, associated with previous results [12] providing an explicit form of the Safety Factor, Figure 9a). Used in a reverse way, the above leads to determine constraints to be satisfied between gradations, slopes, and heights in designed works, in order to keep the Safety Factor at a given standard level - e.g. Fs=1,50 , reference in usual safety regulations- Figure 9b).

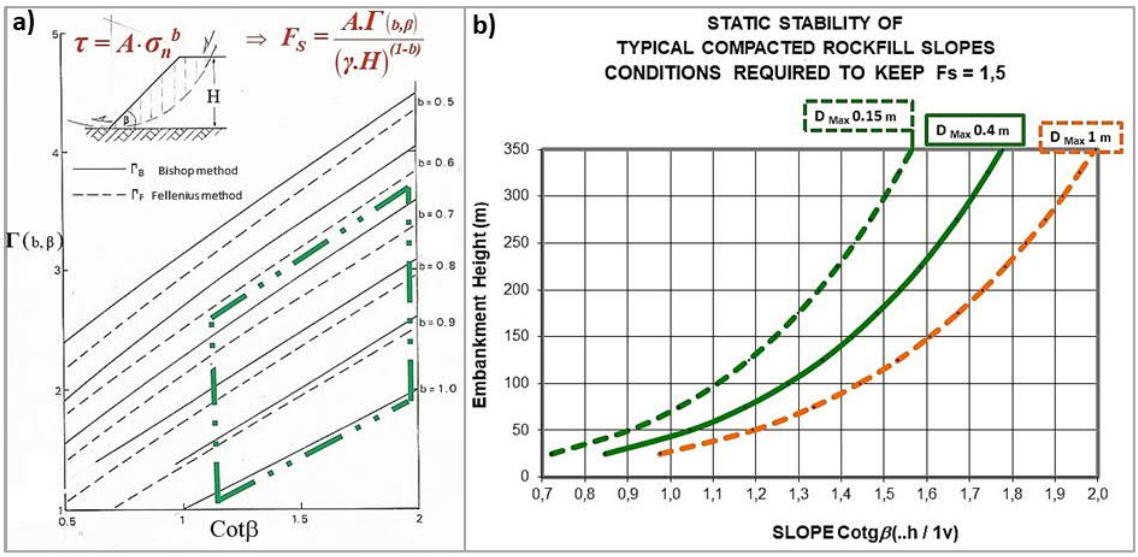

Figure 9 – Explicit scale effects in slope stability against shear failure

It has been shown that the Scale Effect Rule applies also to deformations, and to the "*apparent rigidity modulus*" of granular geomaterials, provided that above similarity conditions are respected:

$$E_1 \approx E_0 \cdot \left(D_1 / D_0 \right)^{-3/m} \qquad (18)$$

This relation, confirmed by independent data on a wide set of well documented large embankments, allows to explain [1] a large part of the serious incidents reported in the paper introduction.

Concluding remarks

In the spirit of these typical models of standard material behaviours in Engineering Sciences, which have proved in the past to be so useful in Hydraulics, Physics of Gases, Mechanics of Materials in Structural Analysis, etc., the development of some kind of "ideal granular material" with direct practical applications, capturing the key features of mechanical behaviour with very few relevant physical parameters, would be of great use in Civil Engineering.
The set of results displayed in the paper show that it can be reached by a better integration of true micro-scale materials physics within macro-scale constitutive models.

References

[1] E. Frossard, Granular Geomaterials Dissipative Mechanics-Theory and Applications in Civil Engineering, ISTE Ltd-J. Wiley & Sons, 308 p., ISBN 978-1-78630-264-9, Oct 2018
[2] W.J.M. Rankine, On the stability of loose earth, *Philosophical Transactions of the Royal Society of London*, Part 1, Vol.**147**,*9-27*, 1857
[3] I. Prigogine, Introduction to thermodynamics of irreversible processes, J. Wiley & Sons, New York, 1968
[4] E. Frossard, Dilatance, dissipation d'énergie et critère de rupture tridimensionnel dans les matériaux granulaires, *Revue Française de Géotechnique*, n° 34, 17-31, Paris, 1986
[5] S. Nemat-Nasser, N. Okada, Radiographic and microscopic observation of shear bands in granular materials, *Géotechnique* **51**, N°9, 753-765, London, 2001
[6] C.A. Coulomb, Essai sur une application des règles de maximis et minimis à quelques problèmes de statique relatifs à l'architecture, *Mémoires Présentés à l'Académie Royale des Sciences par Divers savants*, Vol. **7**, 343-382, Paris, 1773
[7] A. Casagrande, Characteristics of Cohesionless Soils Affecting the Stability of Slopes and Earth Fills, *Journal of Boston Society of Civil Engineers*, Vol. 23, N°1 ,13-32, 1936
[8] P.V. Lade, J.M. Duncan, Cubical triaxial tests on cohesionless soil, *ASCE Journal of the Soil Mechanics and Foundation Division*, **99** (10), 793-812, New-York, 1973
[9] P.W. Rowe, The Stress-Dilatancy Relation for Static Equilibrium of an Assembly of Particles in Contact, *Proceedings Royal Society*, Series A, 269, 500–527, London, 1962
[10] T.B.S. Pradhan, F. Tatsuoka, Y. Sato, Experimental stress-dilatancy relations of sand subjected to cyclic loading, *Soils and Foundations*, Vol.29, n° 1, 45-64, Japanese Geotechnical Society, Tokyo, 1989
[11] E. Frossard, W. Hu, C. Dano, P.Y. Hicher, Rockfill shear strength evaluation: a rational method based on size effects, *Géotechnique* **62**, N°5, 415-427, London, 2012
[12] J.A. Charles, N.M. Soares, Stability of Compacted Rockfill Slopes, *Géotechnique*, Vol.34, n°1, 61-70, 1984 -*See also* J.A. Charles, Laboratory shear strength tests and the stability of rockfill slopes, *in Advances in Rockfill Structures -Ed by E. Maranha das Neves*– Kluwer Publ., p 53-72, 1990